



OPTIMIZATION FORMULATION OF INSULIN-LOADED POLY-CAPROLACTONE NANOPARTICLES FOR CHRONIC WOUND HEALING USING BOX-BEHNKEN DESIGN

KRONİK YARA İYİLEŞMESİ İÇİN İNSÜLİN YÜKLÜ POLİ-KAPROLAKTON NANOPARTİKÜLLERİNİN BOX-BEHNKEN DENEYSEL TASARIMI KULLANILARAK OPTİMİZASYONU

Tamer TEKİN^{1,2} , Ayşegül YILDIZ¹ , Fatmanur TUĞCU DEMİRÖZ¹ ,
Füsün ACARTÜRK^{1*}

¹Gazi University, Faculty of Pharmacy, Department of Pharmaceutical Technology, 06330, Ankara, Türkiye

²Selçuk University, Faculty of Pharmacy, Department of Pharmaceutical Technology, 42130, Konya, Türkiye

ABSTRACT

Objective: The aim of this study is to optimize the formulation of insulin-loaded poly-caprolactone nanoparticles (INS-PCL-NP) for use in chronic wound healing using Box-Behnken experimental design.

Material and Method: The response of independent variables (poly-caprolactone concentration, polyvinyl alcohol concentration and sonication time) on dependent variables (particle size, PDI and encapsulation efficiency) were evaluated. Nanoparticle formulations were produced by the double emulsion (w/o/w)-solvent evaporation method. The resulting formulations were characterized in terms of particle size, zeta potential, and encapsulation efficiency to determine the optimum formulation. Further analyses, including morphological analyses, Fourier-transform infrared spectroscopy (FTIR), differential scanning calorimetry (DSC), and in vitro drug release studies were conducted on the optimized formulation.

Result and Discussion: According to the results of the characterization studies, it was observed that the optimized nanoparticles had a particle size of 618.5 ± 11.2 nm, a PDI of 0.194 ± 0.021 , a zeta potential of -8.21 ± 1.1 mV and an encapsulation efficiency of $73.1 \pm 4.2\%$. In morphological analysis, it was observed that the nanoparticles had a spherical structure. The optimized nanoparticle formulation showed a rapid release of $49.1 \pm 2.1\%$ within the first 24 hours, followed by a controlled release for 168 hours.

Keywords: Box-Behnken design, insulin, nanoparticle, polycaprolactone

ÖZ

Amaç: Bu çalışmanın amacı kronik yara iyileşmesinde kullanılmak üzere insülin yüklü poli-kaprolakton nanopartiküllerinin (INS-PCL-NP) formülasyonunu Box-Behnken deneysel tasarımı kullanarak optimize etmektir.

Gereç ve Yöntem: Bağımsız değişkenlerin (poli-kaprolakton konsantrasyonu, polivinil alkol konsantrasyonu ve sonikasyon süresi) bağımlı değişkenlere (partikül boyutu, PDI ve kapsülleme verimliliği) tepkisi değerlendirilmiştir. Nanopartikül formülasyonları çift emülsiyon (s/y/s)-çözücü buharlaştırma yöntemi ile üretilmiştir. Optimum formülasyonu belirlemek için nanopartiküller partikül boyutu, zeta potansiyeli ve enkapsülasyon etkinliği açısından karakterize edilmiştir.

* Corresponding Author / Sorumlu Yazar: Füsün Acartürk
e-mail / e-posta: acarturk@gazi.edu.tr, Phone / Tel.: +905323660041

Deneyisel tasarıma uygun olarak belirlenen optimum nanopartikül formülasyonu ile morfolojik analizler, FTIR, DSC analizleri ve in vitro ilaç salım çalışmaları yapılmıştır.

Sonuç ve Tartışma: Karakterizasyon çalışmalarının sonuçlarına göre, optimize edilmiş nanopartiküllerin 618.5 ± 11.2 nm partikül boyutuna, 0.194 ± 0.021 PDI'ye, -8.21 ± 1.1 mV zeta potansiyeline ve $\%73.1 \pm 4.2$ enkapsülasyon etkinliğine sahip olduğu görülmüştür. Morfolojik analizde, nanopartiküllerin küresel bir yapıya sahip olduğu görülmüştür. Optimize edilmiş nanopartikül formülasyonu, ilk 24 saat içinde $\%49.1 \pm 2.1$ 'lik ilk salım, ardından 168 saat boyunca kontrollü salım göstermiştir.

Anahtar Kelimeler: Box-Behnken tasarımı, insülin, nanopartikül, polikaprolakton

INTRODUCTION

Type 2 diabetes mellitus is prevalent worldwide and accounts for more than \$760 billion annually, accounting for 10% of total healthcare expenditures [1]. Chronic foot wounds occur in patients with nerve damage due to diabetes, and the healing of these wounds is a challenging and complex process [2]. Hemostasis, inflammation, proliferation and remodelling are the stages of wound healing [3,4]. Impairments in the healing mechanisms in chronic diabetic wounds lead to a prolonged inflammatory phase, thereby complicating the wound healing process [5].

Growth factors such as beta transforming growth factor (TGF- β) and epidermal growth factor (EGF) have been shown to promote wound healing by accelerating cell migration and proliferation [4,6]. However, the limited stability and high cost of these growth factors constrain their clinical application [7]. Insulin (INS) is a hydrophilic peptide hormone and growth factor primarily responsible for regulating blood glucose levels. However, in recent years, it has also been recognized for its effectiveness in promoting wound healing. Insulin contributes to tissue regeneration by facilitating cellular reconstruction in the wound area. Its pure crystalline form and compatibility with polymers in wound dressings and drug delivery systems enhance its applicability. However, insulin has a short half-life when administered locally, and it has been reported that effective healing in the wound area has been achieved with the controlled release of insulin [8]. Since insulin is a peptide-based protein, it is prone to rapid degradation; therefore, to mitigate this issue, it must be encapsulated within a suitable carrier system to enhance its stability and bioavailability [9]. Insulin encapsulated polymeric nanoparticles was found to be effective and stable in wound healing in diabetic rat [8,10].

Polymeric nanoparticles are drug delivery systems that can be produced from synthetic/natural polymers and typically range in size from 10-1000 nm. Insulin encapsulation in biocompatible and biodegradable polymers such as poly-caprolactone (PCL), poly-lactide-co-glycolide (PLGA), poly-lactic acid (PLA), is a common strategy [11,12]. PCL is a commonly used polymer in nanoparticle production, owing to its advantageous properties, including its biocompatibility, biodegradability, and the absence of inflammatory responses during degradation [13].

Many methods have been developed for the production of polymeric nanoparticles. Various methods have been used in the production of PCL nanoparticles, such as solvent evaporation-emulsification, nanoprecipitation and solvent displacement [14]. The double emulsion-solvent evaporation method is widely applied in the encapsulation of water-soluble proteins, and this method provides long-term drug release and high encapsulation efficiency [9].

In our study, the optimum PCL nanoparticle formulation for insulin encapsulation was prepared by the double emulsion-solvent evaporation method. We aimed to develop insulin-loaded PCL nanoparticle (INS-PCL-NP) through a design of experiments approach. A Quality by Design (QbD) approach was performed to understand the interactions on the desired properties in insulin-loaded PCL nanoparticle formulations and to obtain optimum nanoparticle. For this purpose, Box-Behnken experimental design was used to optimize formulation parameters and investigate the effect of independent variables (PCL concentration, polyvinyl alcohol (PVA) concentration and sonication time) on dependent variables (particle size, polydispersity index (PDI) and encapsulation efficiency).

MATERIALS AND METHODS

Materials

Poly-caprolactone (MW: 45.000 Da), polyvinyl alcohol (MW: 25.000 Da), dichloromethane (DCM), sorbitan monooleate 80 (Span 80) and recombinant human insulin were supplied by Sigma Aldrich. Sodium sulfate was supplied by Zag Chemistry. HPLC grade acetonitrile was supplied by Merck. Water was produced using reverse osmosis (Milli-Q, Milipore). All other reagents and solvents were of analytical grade.

Preparation of Nanoparticles

The water-oil-water (w/o/w) double emulsion solvent evaporation method was used to prepare INS-PCL-NPs. During the process, 10 ml of DCM solution containing 250 mg of Span 80 and PCL at varying ratios (1-2.5% w/v) was mixed for the preparation of the organic phase. Then, 1 ml of insulin solution (1 mg/ml) was added dropwise into the organic phase and emulsified by sonication for 60 sec using an ultrasound probe (Vibra cell, BioBlock Scientific, Strasbourg, France) at 60 amplitude and 50 W output amplitude to form the primary emulsion (w/o). The primary emulsion was then added dropwise into 40 ml of an aqueous PVA solution (0.1-0.3%) and emulsified by sonication under the same conditions for varying times (30-90 sec) to form the double emulsion (w/o/w). After the organic phase was removed by rotary evaporator, the nanoparticles were centrifuged at 15000 rpm for 20 min. The precipitated nanoparticles were re-dispersed in 3 ml of water and frozen at -80°C before lyophilization.

Box-Behnken Experimental Design

The Box-Behnken design was used to obtain the optimized INS-PCL-NP formulation using 13 trials created on 3 independent and 3 dependent variables with Design Expert (Version 13.0.5.0, Stat-Ease Inc., Minneapolis, Minnesota). Response surface plots and second-order polynomial models with three factors at three levels were generated for the design [15,16]. In the preliminary formulation studies, the effects of PCL concentration (%) (X_1), PVA concentration (X_2) and sonication time (s) (X_3) were evaluated assigning low, medium, and high levels to each parameter. The objective was to formulate nanoparticles with an average particle size of approximately 600 nm, which would enable high encapsulation efficiency and prolonged controlled release. The dependent and independent variables are shown in Table 1. The polynomial equation derived from the experimental data is presented as follows:

$$Y = A_0 + A_1X_1 + A_2X_2 + A_3X_3 + A_4X_1X_2 + A_5X_1X_3 + A_6X_2X_3 + A_7X_1^2 + A_8X_2^2 + A_9X_3^2$$

In the equation here, Y is the response obtained from the dependent variables and A_0 is the intersection point of this response. The regression coefficients of Y are coded between A_1 - A_9 and the values are obtained as a result of experimental studies. The independent variables are expressed as X_1 , X_2 and X_3 . X_i^2 (f = 1, 2, 3) shows the quadratic values and $X_y X_z$ (y, z = 1, 2, 3) shows the interaction values.

Table 1. Box-Behnken design: Dependent and independent variable levels

Independent Variables	Levels		
	-1	0	1
X_1 = PCL concentration (w/v %)	1	1.75	2.5
X_2 = PVA concentration (w/v %)	0.1	0.2	0.3
X_3 = Sonication time (sec)	30	60	90
Dependent Variables	Restrictions		
Y_1 = Average particle size (nm)	600		
Y_2 = PDI	Minimize		
Y_3 = Encapsulation efficiency (%)	Maximize		

Method for Quantification of Insulin

To quantify insulin in the nanoparticle formulations, the Ultra Performance Liquid Chromatography-UV/Visible Spectrophotometry (UPLC-UV) reversed phase method was used. The isocratic system (Waters, Vienna, Austria) was studied and validated using the method performed according to the USP monograph [17]. InertSustain C18 column (150 mm*4.6 mm*2 μ m) (GL Sciences, Tokyo, Japan) was used as the stationary phase and 0.02 M pH 3.1 Na₂SO₄ buffer: acetonitrile (65:35) was used as the mobile phase, and the column temperature was kept constant at 40 °C throughout the analysis. The mobile phase flow rate was kept constant at 0.5 ml/min throughout the analysis and the injection volume was set at 20 μ l. The system consists of a solvent chamber, a processor-controlled high-pressure pump that provides dispersion of the mobile phase and a UV detector with a λ max of 214 nm.

Drug Encapsulation Efficiency

The indirect method was used to calculate the encapsulation efficiency of nanoparticles. After the centrifugation of the nanoparticles at 15000 rpm for 20 minutes (Beckman Coulter, CA, USA), they were washed 3 times, and the supernatants were analyzed with UPLC. After determining the amount of non-encapsulated insulin remaining in the supernatant, the encapsulation efficiency [18] was calculated according to the following equation:

$$\text{Encapsulation efficiency (\%)} = \left(\frac{(\text{Total amount of drug}) - (\text{Amount of free drug})}{\text{Total drug}} \right) \times 100$$

Particle Size, Polydispersity Index and Zeta Potential Measurement

The zeta potential, polydispersity index and particle size properties of the nanoparticles were evaluated using the Zetasizer Nano-ZS90 (Malvern, Worcestershire, England) device, which uses the photon correlation spectroscopic method. All analysis was carried out in three replicates.

Morphological Analysis of Optimized Nanoparticles

Scanning electron microscope (QUANTA 400F Field Emission) was used for morphological analysis of nanoparticles. After the optimized nanoparticle formulation was produced, the suspended samples were dropped onto an aluminum surface and waited for drying. Images were taken at 24000x and 50000x magnification of different parts of the formulations coated with gold/palladium.

Fourier Transform Infrared Spectroscopy (FTIR) Analysis

FTIR spectroscopy with an Attenuated Total Reflectance (ATR) probe was used to analyse insulin, PCL and insulin-loaded PCL nanoparticles (Spectrum 400, Perkin Elmer, USA). All analysis were carried out in the wavelength range of 4000-400 cm⁻¹.

Differential Scanning Calorimetry (DSC) Analysis

DSC analysis (DSC 60, Shimadzu, Japan) of insulin, PCL and insulin-loaded PCL nanoparticles were performed to order to assess possible interactions and structural changes. 2 mg samples were prepared in aluminum pans and heated from 25 °C to 350 °C in nitrogen atmosphere at a rate of 10 °C/min.

In Vitro Drug Release Studies

Release studies of insulin from INS-PCL-NPs were performed using Franz diffusion cells and, in this study, diffusive area was 1 cm² [19]. Dialysis membrane (SERVA, molecular weight cutoff: 12000–14000) was placed between the donor and receptor compartments of the Franz diffusion cell. For the preparation of the simulated wound fluid (SWF) (pH:6.2), 8.298 g of sodium chloride and 0.368 g of calcium chloride were dissolved in 1 l of distilled water [20]. The re-dispersed nanoparticle suspension (50 mg/ml) was placed in the donor compartment and the receptor compartment containing simulated wound fluid thermostated at 37°C. The samples were taken from the receptor phase at the predetermined

time intervals and fresh SWF added the receptor phase at the same volume. The samples were analyzed using UPLC-UV to calculate the drug release. Using in vitro release data, the release kinetics of insulin from INS-PCL-NPs were evaluated for compatibility with the zero order, first order, Higuchi, Weibull, Hixson-Crowell and Korsmeyer-Peppas kinetic models using DDSolver[®] software.

RESULT AND DISCUSSION

Experimental Analysis

In order to optimize nanoparticle formulation, 13 confirmatory trials with 1 center point including 3 independent and 3 dependent variables were performed according to Box-Behnken design for nanoparticle production. The independent variables used for nanoparticle production are shown in Table 2. Nanoparticle formulations were characterized in terms of the particle size, polydispersity index, encapsulation efficiency and zeta potential and the results are given in Table 2. Response-surface graphs were created by the Design-Expert software to evaluate the effects of independent variables on dependent variables.

Table 2. The results of the Box-Behnken design

Formulation	Independent variables			Dependent variables			
	PCL concentration (%)	PVA concentration (%)	Sonication time (sec)	Particle size (nm)	PDI	Encapsulation efficiency (%)	Zeta potential (mV)
1	1	0.1	60	438.4 ± 12.2	0.283 ± 0.034	42.1 ± 7.4	-1.3 ± 1.1
2	1	0.2	30	276.4 ± 4.2	0.212 ± 0.031	46.9 ± 11.3	-10.3 ± 3.3
3	1	0.2	90	286.2 ± 4.5	0.179 ± 0.014	77.8 ± 4.3	-10.9 ± 2.8
4	1	0.3	60	244.6 ± 6.7	0.156 ± 0.017	79.8 ± 5.9	-7.7 ± 2.6
5	1.75	0.1	30	478.1 ± 6.4	0.141 ± 0.011	42.2 ± 4.9	-9.8 ± 4.1
6	1.75	0.1	90	618.5 ± 9.1	0.194 ± 0.011	53.3 ± 7.2	-2.6 ± 8.1
7	1.75	0.2	60	309.6 ± 4.9	0.189 ± 0.089	78.6 ± 8.1	-8.5 ± 2.6
8	1.75	0.3	30	309.8 ± 3.5	0.171 ± 0.021	39.2 ± 6.1	-8.3 ± 4.9
9	1.75	0.3	90	262.4 ± 2.1	0.188 ± 0.014	44.7 ± 9.2	-0.8 ± 0.1
10	2.5	0.1	60	498.8 ± 6.4	0.119 ± 0.052	71.3 ± 3.1	-1.2 ± 0.9
11	2.5	0.2	30	645.9 ± 7.3	0.376 ± 0.091	57.4 ± 10.2	-11.6 ± 7.1
12	2.5	0.2	90	288.8 ± 3.9	0.174 ± 0.011	66.6 ± 7.7	-11.6 ± 8.1
13	2.5	0.3	60	294.3 ± 3.1	0.213 ± 0.016	73.1 ± 4.4	-0.9 ± 0.3

Zeta Potential Measurements

Zeta potential is a value that allows the electrostatic charges on the surface to estimate the repulsive forces between the particles and provides information about the stability of the nanoparticles [18]. As a result of the zeta potential measurements, the main effect on the surface charge was considered to be PCL and it provided the nanoparticles to be anionic owing to its negative structure [21]. The surface charges of nanoparticles were found to be negative and between -0.8 ± 0.1 and -11.6 ± 8.1 mV. The physical stability of nanoparticles is strongly influenced by their zeta potential. At high absolute zeta potential values, particles repel each other, reducing the likelihood of aggregation and indicating good stability. Conversely, at low absolute zeta potential values, repulsive forces are insufficient to prevent aggregation, leading to potential instability during long-term storage. Therefore, the relatively low zeta potential values observed suggest that the nanoparticles may exhibit limited physical stability over extended storage periods. The data obtained from the optimized nanoparticles are shown in Figure 1. In addition, the zeta potential was not included in the dependent variables since the pre-formulation studies showed that no significant changes in the zeta potential occurred with changes in the independent parameters.

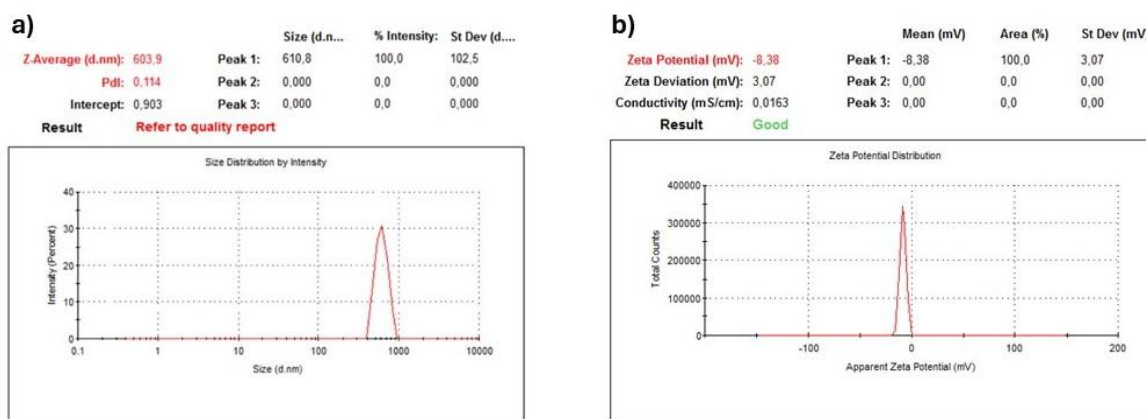


Figure 1. a) Size distribution, b) Zeta potential of optimum drug-loaded PCL nanoparticle

Effect of Independent Variables on Particle Size

The particle size of the nanoparticles was found to be between 262.4 ± 2.1 - 618.5 ± 9.1 nm (Table 2).

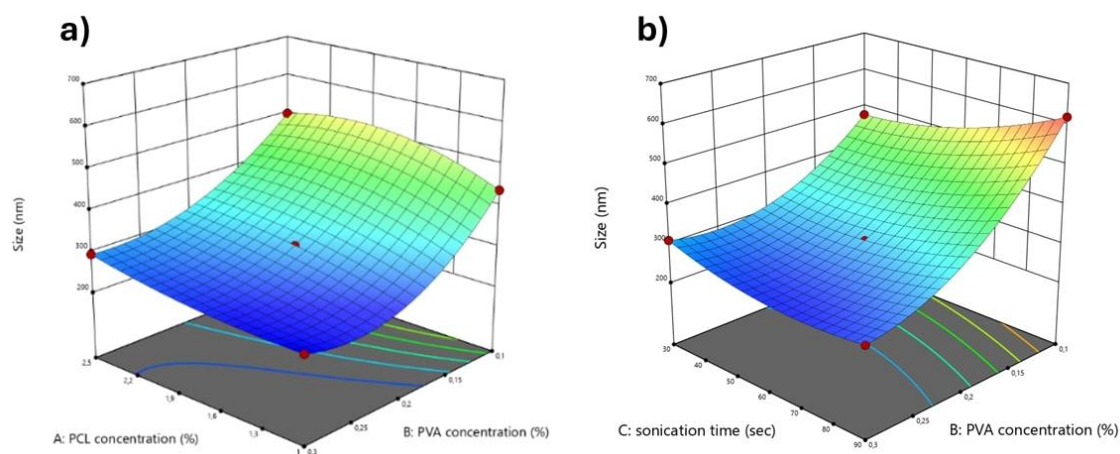


Figure 2. Surface plots presenting the effect of a) PCL and PVA concentration and b) sonication time and PVA concentration on particle size

The second-degree polynomial equation showing the effects on particle size (Y_1) is given below:

$$Y_1 = 309.6 + 35.33X_1 - 115.39X_2 - 6.84X_3 - 2.89X_1X_2 - 41.75X_1X_3 - 47.075X_2X_3 - 16.7125X_1^2 + 76.0125X_2^2 + 31.4625X_3^2$$

The negative coefficients in the obtained polynomial equation indicate antagonistic effects, whereas the positive coefficients indicate synergistic effects. A quadratic model was proposed in the design, and the R^2 and adjusted R^2 values were determined as 0.7270 and 0.6227, respectively. Since R^2 values above 0.5 are generally considered acceptable, these results suggest that the model provides a reasonable fit and the design is reliable [21]. The signal-to-noise ratio was found to be 7.059, which exceeds the threshold of 4, indicating suitability for navigation in the design area [18]. Polymer concentration influences the particle size and the size affects the drug release behavior along with the matrix behavior. The generated polynomial equation clearly indicates that the PCL concentration (X_1) has a positive effect on particle size, meaning that an increase in polymer concentration results in larger

particles (Figure 2a). This can be attributed to the increase in the viscosity of the organic phase during sonication as the polymer concentration increases, leading to the formation of larger particles. The sonication time (X_3) applied to the secondary emulsion was found to influence the size of the nanoparticles. Longer sonication times resulted in a reduction in nanoparticle size, suggesting that the increase in energy transferred during the sonication process facilitated the formation of smaller particles. This effect can be attributed to the enhanced shear forces exerted during prolonged sonication, which promote the fragmentation of larger aggregates into smaller, more uniform particles [22]. It was observed that the PVA concentration (X_2) had an inverse relationship with particle size, meaning that an increase from 0.1% to 0.3% resulted in a decrease in particle size (Figure 2b). This suggests that the PVA concentration plays a crucial role in controlling nanoparticle size. However, both excessively high and low stabilizer concentrations can lead to aggregation and clustering, highlighting the importance of using the optimal PVA concentration.

Effect of Independent Variables on PDI

Due to the low coefficients of the independent variables obtained from the polynomial equation, it was interpreted that the independent variables had a low effect on the PDI.

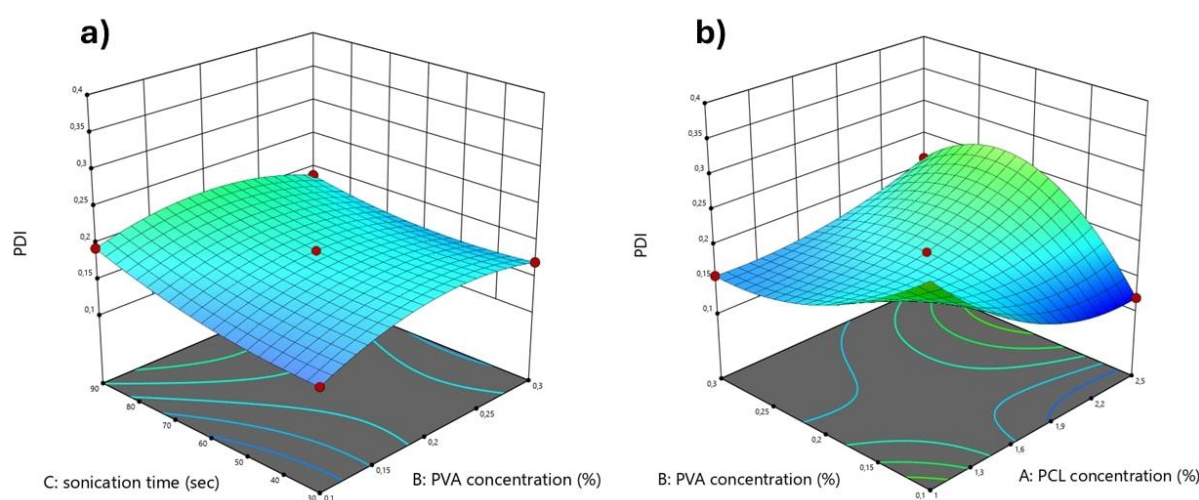


Figure 3. Surface plots presenting the effect of a) sonication time and PVA concentration and b) PCL and PVA concentration on PDI

The second order polynomial equation showing the effects on PDI (Y_2) is given below.

$$Y_2 = 0.189 + 0.03975X_1 + 0.00625X_2 + 0.01775X_3 + 0.05525X_1X_2 - 0.04225X_1X_3 - 0.00925X_2X_3 + 0.032875X_1^2 - 0.029125X_2^2 + 0.013375X_3^2$$

The R^2 value obtained from the polynomial equation was found to be 0.6008. It was found that there was a direct correlation between PCL concentration (X_1) and PDI, where a slight increase in PDI was observed with an increase in PCL concentration (Figure 3b). It was observed that the sonication time (X_2) applied to the secondary emulsion had a low positive effect on PDI though this effect was not remarkable. Additionally, the PVA concentration (X_3) showed a low positive effect on PDI, suggesting that higher stabilizer concentrations may lead to aggregation (Figure 3a). Additionally, the PDI values of the produced nanoparticles were generally found to be less than 0.3. Low PDI values indicate that the produced particles have high stability and are not prone to aggregation [23].

Effect of Independent Variables on Encapsulation Efficiency

Independent variables were found to have low effects on encapsulation efficiency.

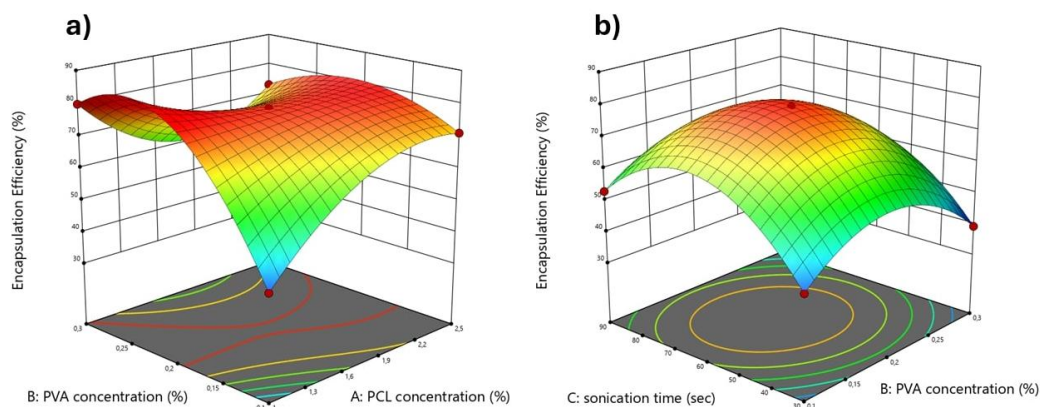


Figure 4. Surface plots presenting the effect of a) PCL and PVA concentration and b) sonication time and PVA concentration on encapsulation efficiency

$$Y_3 = 78.6 - 0.3X_1 - 2.75X_2 + 4.15X_3 - 8.95X_1X_2 - 5.3X_1X_3 - 1.25X_2X_3 + 2.55X_1^2 - 14.7X_2^2 - 19.05X_3^2$$

The R^2 value obtained from the polynomial equation was found to be 0.6444. A slight negative effect is observed on encapsulation efficiency with increasing PCL concentration (Figure 4a). Similarly, a negative effect on encapsulation was noted with an increase in PVA concentration. Conversely, a slight positive effect on encapsulation was observed with increasing sonication time (Figure 4b). Overall, no significant effect of the independent variables on encapsulation efficiency was detected.

UPLC-UV Method for Quantification of Insulin

The calibration curve was created for nine different concentrations between 5-45 $\mu\text{g/ml}$. The regression equation and correlation coefficient were calculated using the graph between peak area and concentration. The linear regression equation for insulin was found as $y = 153211x + 91246$. The coefficient of determination defined as r^2 was used to evaluate the linearity of the calibration line. The linearity of the graph increases as the r^2 value approaches 1. The correlation coefficient was found as $r^2 = 0.9966$ for INS and a correlation was observed between the peak areas and drug concentrations. The calibration line showed that UPLC is a sensitive method for insulin quantification and an effective analysis technique to accurately determine the active substance content in nanoparticles. The calibration curve for insulin is shown in Figure 5.

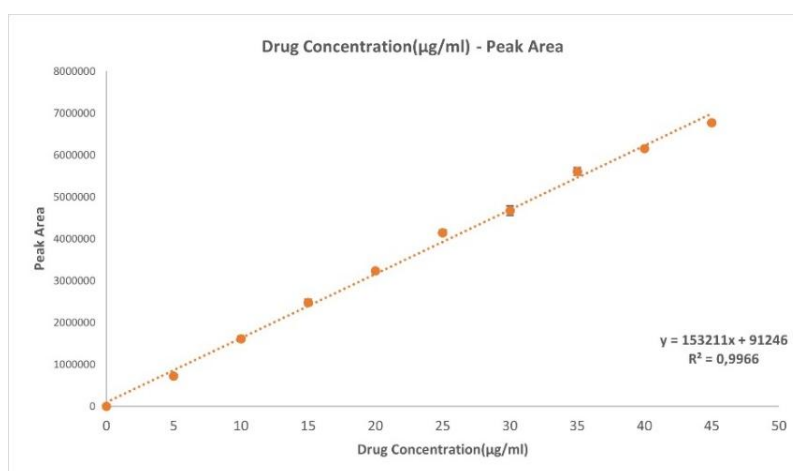


Figure 5. Calibration curve of insulin

Production of Optimized INS-PCL-NPs

The parameters required for optimum INS-PCL-NP production were determined by applying the constraints in Table 1 to the dependent factors. Point estimation was used in Design Expert software and the desirability value close to 1 is accepted in other studies [18]. According to the predictions of the software, the optimum nanoparticle formulations with a desirability value of 0.741 will be obtained with the parameters $X_1 = 2.5\%$, $X_2 = 0.15\%$ and $X_3 = 50$ s and the following responses will be obtained: $Y_1 = 588.7$ nm, $Y_2 = 0.2$ and $Y_3 = 79.8\%$. Optimized INS-PCL-NP formulations were generated and the role of the polynomial equation generated by the software in predicting the responses was investigated. Experimental results confirmed that the optimized formulations were in good agreement with the model (Table 3), giving values of $Y_1 = 618.5 \pm 11.2$ nm, $Y_2 = 0.194 \pm 0.021$ and $Y_3 = 73.1 \pm 4.2\%$ [24]. The zeta potential of the optimized nanoparticles was found to be -8.21 ± 1.1 mV. In a study conducted by Socha et al., insulin-containing PCL nanoparticles were produced using the w/o/w method, and 519.9 ± 34.5 nm size and $95.4 \pm 1.5\%$ encapsulation efficiency were obtained using 2.5% PCL concentration, 60 seconds sonication time and 0.1% PVA concentration in nanoparticle production. In addition, in the same study, PCL nanoparticles were found to have a negative zeta potential value (-9.5 ± 4.9 mV) as in our study [12]. In another study insulin loaded nanoparticles were produced using the w/o/w method, Pluronic F68 was used as a stabilizer, and according to the characterization studies nanoparticles had a particle size of 796 ± 10.5 nm, a PDI of 0.49 ± 0.06 , an encapsulation efficiency of $90.6 \pm 1.6\%$, and a zeta potential of 29.4 ± 2.7 mV. A thorough examination of these studies reveals that the nanoparticles obtained exhibit greater uniformity in size, attributable to their low PDI value. This observation lends credence to the efficacy of the applied factorial design.

Table 3. Optimum parameters of INS-PCL-NP formulation produced with the independent variables suggested by the Box-Behnken design

PCL concentration (%)	PVA concentration (%)	Sonication time (sec)	Particle size (nm)	PDI	Encapsulation efficiency (%)
2.5	0.15	50	618.5 ± 11.2	0.194 ± 0.021	73.1 ± 4.2

Scanning Electron Microscope (SEM) Analysis

The SEM image of the optimized INS-PCL-NP formulation is shown in Figure 6. It was observed that the nanoparticles had a near-spherical shape, with some particles connected at specific points by surface bridges. This is likely due to the adhesive properties of PVA, which can promote particle interaction and aggregation. These surface bridges imply that PVA not only functions as a stabilizer for the nanoparticles but also influences their morphological characteristics by promoting interparticle interactions [25]. In a study by Iqbal et al., PCL nanoparticles were prepared by the w/o/w method and PVA was used as a stabilizer. In the morphological analysis in the study, it was observed that PVA had an adhesive effect on the particles, similar to our study [26].

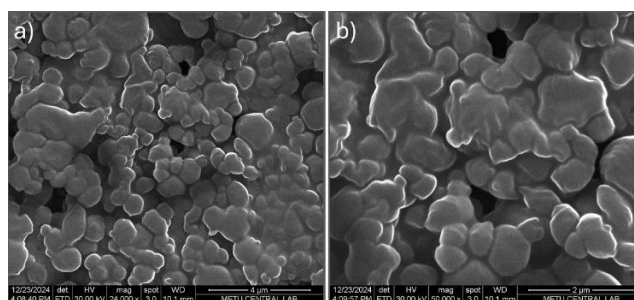


Figure 6. Scanning electron microscope image of optimized INS-PCL-NPs at a) 24000x and b) 50000x magnifications

Fourier Transform Infrared Spectroscopy (FTIR) Analysis

The FTIR spectra of insulin, PCL and INS-PCL-NP are shown in Figure 7. In the spectrum of insulin in Figure 7a, Amide I, Amide II and Amide III bands are seen. The Amide I band between 1700-1600 cm^{-1} is assigned to the stretching of the carbonyl groups in the protein backbone ($\text{C}=\text{O}$). The Amide II band, observed between 1580-1500 cm^{-1} , arises from the combination of NH and CN vibrations. The amide III band, which occurs within the range of 1350-1200 cm^{-1} , has been identified as being associated with the coupling of CN and NH vibrations. These bands have been identified as characteristic of insulin and have been found to be in accordance with the existing literature [27]. In the FTIR spectrum of PCL in Figure 7b, the symmetric aliphatic stretching is seen at 2868 cm^{-1} , the asymmetric aliphatic stretching is seen at 2944 cm^{-1} , the characteristic carbonyl ($\text{C}=\text{O}$) stretching band is seen at 1724 cm^{-1} , the C–O and C–C stretching vibration bands are seen at 1292 cm^{-1} and the symmetric C–O–C and asymmetric C–O–C vibration bands are seen at 1164 and 1236 cm^{-1} , respectively. In a study, indomethacin-loaded PCL nanoparticles were produced. According to the results of the FTIR analysis, it was seen that the characteristic bands of PCL were similar to our FTIR data [28]. In the spectrum of insulin-loaded nanoparticles, the characteristic amide bands of insulin almost completely disappeared, and no distinct peaks were observed in this spectrum (Figure 7c). This indicates that insulin was successfully encapsulated in PCL nanoparticles.

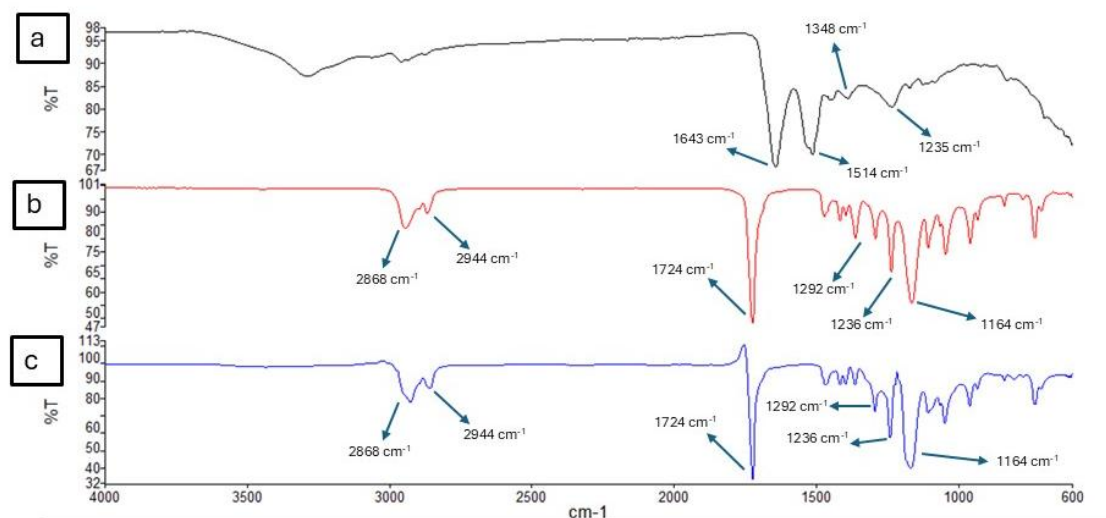


Figure 7. FTIR spectra of a) Insulin, b) PCL, c) INS-PCL-NP

Differential Scanning Calorimetry Analysis

DSC thermograms of insulin, PCL and INS-PCL-NP are shown in Figure 8. As demonstrated in Figure 8a, the DSC thermograms revealed that PCL demonstrated an endothermic peak at 61 °C. This occurrence was ascribed to the presence of its crystalline structure. Furthermore, this peak was found to be in accordance with the findings reported by Badri et al. [28]. As demonstrated in Figure 8b, insulin exhibited a small endothermic peak at 214 °C. The resulting thermogram was found to be in accordance with the thermogram obtained by Zhao et al [29]. In the thermogram of INS-PCL-NP, the endothermic peak corresponding to PCL was observed; however, the peak associated with insulin was not detected (Figure 8c). This absence is thought to be due to a decrease in the amount of insulin in the nanoparticle, possibly as a result of encapsulation within the particles.

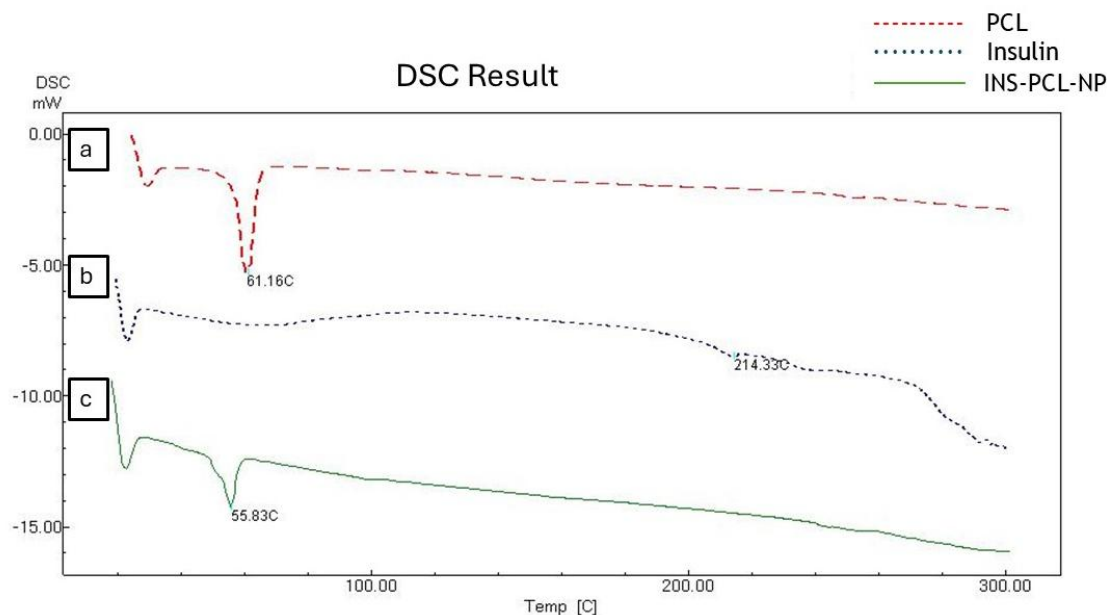


Figure 8. DSC thermograms of a)PCL, b)insulin and c)INS-PCL-NP

***In Vitro* Drug Release Study**

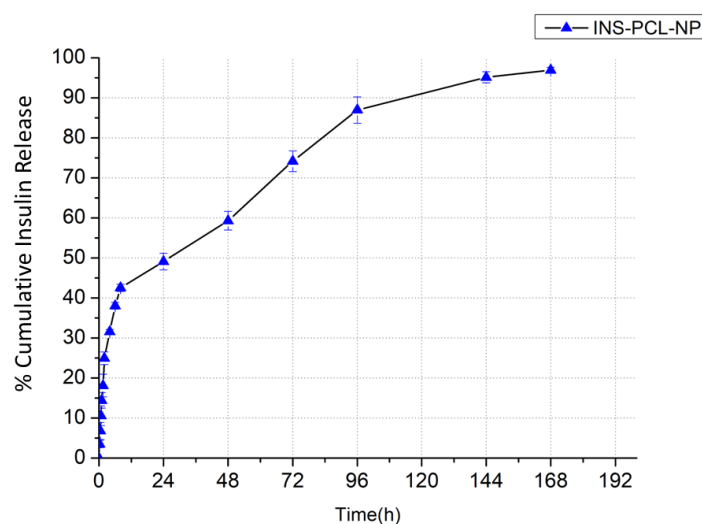
The *in vitro* drug release behavior of INS-PCL-NPs was evaluated. A release of $49.11 \pm 2.01\%$ insulin was observed within the first 24 hours from the optimized INS-PCL-NPs. This rapid release is likely attributed to the insulin present on the surface of the nanoparticles. The nanoparticles released a total of $96.09 \pm 0.73\%$ insulin (Figure 9) at the end of 168 hour. Insulin release is presumed to occur through a diffusion-controlled mechanism. This controlled release is essential for ensuring the sustained therapeutic effect. In a study, cilnidipine loaded PCL nanoparticles were produced and as a result of *in vitro* release study, it was observed that approximately 60% cumulative drug release was obtained at the end of 72 hours [30]. In another study hydrophilic hydroxyurea substance was encapsulated in PCL nanoparticles and showed approximately 34% cumulative drug release at the end of 48 hours [31]. In addition, in a study conducted by Kumar and Sawant, exemestane loaded PCL nanoparticles showed approximately 71% cumulative drug release at the end of 240 hours [32]. According to the results of this study, it was seen that PCL nanoparticles were preferred in controlled drug release, and these studies confirmed our results.

In kinetic modeling, an R^2 value close to 1 indicates that the model is suitable for the release behavior. However, since the R^2 value increases with the addition of the variables and causes inaccurate interpretation of the release profiles. In order to prevent this situation, the R^2_{adj} value is used instead of R^2 [33]. In Table 4, it is seen that the Weibull kinetics has the highest R^2_{adj} value with 0.9625. The AIC is the compatibility parameter. A lower value indicates that the formulation release is suitable for use with the kinetic model. The Weibull model was found to have the lowest AIC value with 106.5018. The MSC parameter is known as the model selection criterion and obtained by normalization of the AIC value. A higher MSC value indicates that the model is highly compatible [34]. The highest MSC parameter among the kinetic models was observed in the Weibull model with a value of 2.9444. The findings of the analysis indicate that the kinetic model that most accurately describes the release of insulin from INS-PCL-NPs is the Weibull model. The Weibull model is a kinetic model that is often highly suitable for polymeric matrix-type structures, such as polymeric nanoparticles [35]. The release of insulin from INS-PCL-NPs initiated rapidly and proceeded in a controlled manner, following Weibull kinetics.

Table 4. Assessment of drug release from INS-PCL-NP formulation based on different kinetic models

Mathematical model	Parameters		Mathematical model	Parameters	
Zero order	R ²	0.5088	Korsmeyer-Peppas	R ²	0.9346
	R ² _{adj}	0.5389		R ² _{adj}	0.9299
	AIC	144.9291		AIC	115.6884
	MSC	0.5427		MSC	2.3702
First order	R ²	0.8363	Hixson-Crowell	R ²	0.7956
	R ² _{adj}	0.8363		R ² _{adj}	0.7956
	AIC	128.3599		AIC	131.9117
	MSC	1.5783		MSC	1.3563
Higuchi	R ²	0.9136	Weibull	R ²	0.9675
	R ² _{adj}	0.9136		R ² _{adj}	0.9625
	AIC	118.1306		AIC	106.5018
	MSC	2.2176		MSC	2.9444

R²: Correlation coefficient, R²_{adj}: Adjusted correlation coefficient, MSC: Model selection criterion, AIC: Akaike information criterion

**Figure 9.** *In vitro* drug release profile of INS-PCL-NPs (n=3)

Conclusion

In this study, insulin-loaded polycaprolactone nanoparticles (INS-PCL-NPs) were successfully developed and optimized for controlled drug delivery in chronic wound healing using the Box-Behnken experimental design. The effects of three independent formulation parameters - PCL concentration, PVA concentration, and sonication time - on key nanoparticle characteristics such as particle size, polydispersity index (PDI), and encapsulation efficiency were systematically investigated. The optimal formulation ($X_1 = 2.5\%$, $X_2 = 0.15\%$, $X_3 = 50$ sec) demonstrated favorable physicochemical properties, including a desirable particle size, narrow size distribution, and high encapsulation efficiency. *In vitro* release studies revealed a biphasic insulin release profile characterized by an initial burst release of approximately 49% within the first 24 hours, followed by a sustained release over 168 hours. Drug release kinetics were best described by the Weibull model, indicating a diffusion-controlled mechanism. Overall, the Box-Behnken design proved to be a valuable tool in the rational development of polymeric

nanoparticle formulations. The optimized INS-PCL-NPs exhibit promising potential for enhancing wound healing in chronic diabetic wounds through sustained and localized insulin delivery.

ACKNOWLEDGEMENTS

This study was supported by Gazi University Scientific Research Projects Unit with project number TGA-2023-8155.

AUTHOR CONTRIBUTIONS

Concept: T.T., A.Y., F.T.D., F.A.; Design: T.T., A.Y., F.T.D., F.A.; Control: F.T.D., F.A.; Sources: F.T.D., F.A.; Materials: F.T.D., F.A.; Data Collection and/or Processing: T.T., A.Y.; Analysis and/or Interpretation: T.T., A.Y., F.T.D., F.A.; Literature Review: T.T., A.Y.; Manuscript Writing: T.T., A.Y., F.T.D., F.A.; Critical Review: T.T., A.Y., F.T.D., F.A.; Other: -

CONFLICT OF INTEREST

The authors declare that there is no real, potential, or perceived conflict of interest for this article.

ETHICS COMMITTEE APPROVAL

The authors declare that the ethics committee approval is not required for this study.

REFERENCES

- Holl, J., Kowalewski, C., Zimek, Z., Fiedor, P., Kaminski, A., Oldak, T., Moniuszko, M., Eljaszewicz, A. (2021). Chronic diabetic wounds and their treatment with skin substitutes. *Cells*, 10(3), 655. [\[CrossRef\]](#)
- Buch, P.J., Chai, Y., Goluch, E.D. (2019). Treating polymicrobial infections in chronic diabetic wounds. *Clinical Microbiology Reviews*, 32(2), 10-1128. [\[CrossRef\]](#)
- Wang, J., Xu, J. (2020). Effects of topical insulin on wound healing: A review of animal and human evidences. *Diabetes, Metabolic Syndrome and Obesity*, 719-727. [\[CrossRef\]](#)
- Oryan, A., Alemzadeh, E. (2017). Effects of insulin on wound healing: A review of animal and human evidences. *Life Sciences*, 174, 59-67. [\[CrossRef\]](#)
- Reiber, G.E., McDonell, M.B., Schleyer, A.M., Fihn, S.D., Reda, D.J. (1995). A comprehensive system for quality improvement in ambulatory care: Assessing the quality of diabetes care. *Patient Education and Counseling*, 26(1-3), 337-341. [\[CrossRef\]](#)
- Tanaka, A., Nagate, T., Matsuda, H. (2005). Acceleration of wound healing by gelatin film dressings with epidermal growth factor. *Journal of Veterinary Medical Science*, 67(9), 909-913. [\[CrossRef\]](#)
- Hrynyk, M., Neufeld, R.J. (2014). Insulin and wound healing. *Burns*, 40(8), 1433-1446. [\[CrossRef\]](#)
- Ribeiro, M.C., Correa, V.L.R., da Silva, F.K.L., Casas, A.A., das Chagas, A.D.L., de Oliveira, L.P., Miguel, M.P., Diniz, D.G.A., Amaral, A.C., de Menezes, L.B. (2020). Wound healing treatment using insulin within polymeric nanoparticles in the diabetes animal model. *European Journal of Pharmaceutical Sciences*, 150, 105330. [\[CrossRef\]](#)
- Iqbal, M., Zafar, N., Fessi, H., Elaissari, A. (2015). Double emulsion solvent evaporation techniques used for drug encapsulation. *International Journal of Pharmaceutics*, 496(2), 173-190. [\[CrossRef\]](#)
- Abdelkader, D.H., Tambuwala, M.M., Mitchell, C.A., Osman, M.A., El-Gizawy, S.A., Faheem, A.M., El-Tanani, M., McCarron, P.A. (2018). Enhanced cutaneous wound healing in rats following topical delivery of insulin-loaded nanoparticles embedded in poly (vinyl alcohol)-borate hydrogels. *Drug Delivery and Translational Research*, 8, 1053-1065. [\[CrossRef\]](#)
- de Araújo, T.M., Teixeira, Z., Barbosa-Sampaio, H.C., Rezende, L.F., Boschero, A.C., Durán, N., Höehr, N.F. (2013). Insulin-loaded poly (ϵ -caprolactone) nanoparticles: Efficient, sustained and safe insulin delivery system. *Journal of Biomedical Nanotechnology*, 9(6), 1098-1106. [\[CrossRef\]](#)
- Socha, M., Sapin, A., Dange, C., Maincent, P. (2009). Influence of polymers ratio on insulin-loaded nanoparticles based on poly- ϵ -caprolactone and Eudragit® RS for oral administration. *Drug Delivery*, 16(8), 430-436. [\[CrossRef\]](#)
- El Yousfi, R., Brahmi, M., Dalli, M., Achalhi, N., Azougagh, O., Tahani, A., Touzani, R., El Idrissi, A. (2023). Recent advances in nanoparticle development for drug delivery: A comprehensive review of polycaprolactone-based multi-arm architectures. *Polymers*, 15(8), 1835. [\[CrossRef\]](#)

14. Byun, Y., Hwang, J.B., Bang, S.H., Darby, D., Cooksey, K., Dawson, P.L., Park, H.J., Whiteside, S. (2011). Formulation and characterization of α -tocopherol loaded poly ϵ -caprolactone (PCL) nanoparticles. *Lwt-Food Science and Technology*, 44(1), 24-28. [\[CrossRef\]](#)
15. Shaikh, M.V., Kala, M., Nivsarkar, M. (2017). Formulation and optimization of doxorubicin loaded polymeric nanoparticles using Box-Behnken design: *Ex-vivo* stability and *in-vitro* activity. *European Journal of Pharmaceutical Sciences*, 100, 262-272. [\[CrossRef\]](#)
16. Gajra, B., Patel, R.R., Dalwadi, C. (2016). Formulation, optimization and characterization of cationic polymeric nanoparticles of mast cell stabilizing agent using the Box–Behnken experimental design. *Drug Development and Industrial Pharmacy*, 42(5), 747-757. [\[CrossRef\]](#)
17. Neumiller, J.J., Chen, G., Newsome, C., Hughes, S., Lazarus, P., White Jr, J.R. (2021). Assessment of regular and NPH insulin concentration via two methods of quantification: the Washington State Insulin Concentration Study (WICS). *Journal of Diabetes Science and Technology*, 15(2), 324-328. [\[CrossRef\]](#)
18. Sharma, D., Maheshwari, D., Philip, G., Rana, R., Bhatia, S., Singh, M., Gabrani, R., Sharma, S.K., Ali, J., Sharma, R.K., Dang, S. (2014). Formulation and optimization of polymeric nanoparticles for intranasal delivery of lorazepam using box-Behnken design: *In vitro* and *in vivo* evaluation. *BioMed Research International*, 2014(1), 156010. [\[CrossRef\]](#)
19. Wissing, S.A., Müller, R.H. (2002). Solid lipid nanoparticles as carrier for sunscreens: *In vitro* release and *in vivo* skin penetration. *Journal of Controlled Release*, 81(3), 225-233. [\[CrossRef\]](#)
20. Khabbaz, B., Solouk, A., Mirzadeh, H. (2019). Polyvinyl alcohol/soy protein isolate nanofibrous patch for wound-healing applications. *Progress in Biomaterials*, 8, 185-196. [\[CrossRef\]](#)
21. Mahmoud, B.S., McConville, C. (2023). Box–Behnken design of experiments of polycaprolactone nanoparticles loaded with irinotecan hydrochloride. *Pharmaceutics*, 15(4), 1271. [\[CrossRef\]](#)
22. Nawaz, T., Iqbal, M., Khan, B. A., Nawaz, A., Hussain, T., Hosny, K.M., Abualsunun, W.A., Rizg, W.Y. (2021). Development and optimization of acriflavine-loaded polycaprolactone nanoparticles using Box–Behnken design for burn wound healing applications. *Polymers*, 14(1), 101. [\[CrossRef\]](#)
23. Romero-Pérez, A., García-García, E., Zavaleta-Mancera, A., Ramírez-Briebesca, J.E., Revilla-Vázquez, A., Hernández-Calva, L.M., López-Arellano, R., Cruz-Monterrosa, R.G. (2010). Designing and evaluation of sodium selenite nanoparticles *in vitro* to improve selenium absorption in ruminants. *Veterinary Research Communications*, 34, 71-79. [\[CrossRef\]](#)
24. Solanki, A.B., Parikh, J.R., Parikh, R.H. (2007). Formulation and optimization of piroxicam proniosomes by 3-factor, 3-level Box-Behnken design. *AAPS Pharmscitech*, 8, 43-49. [\[CrossRef\]](#)
25. Higazy, I.M., Mahmoud, A.A., Ghorab, M.M., Ammar, H.O. (2021). Development and evaluation of polyvinyl alcohol stabilized polylactide-co-caprolactone-based nanoparticles for brain delivery. *Journal of Drug Delivery Science and Technology*, 61, 102274. [\[CrossRef\]](#)
26. Iqbal, M., Valour, J.P., Fessi, H., Elaissari, A. (2015). Preparation of biodegradable PCL particles via double emulsion evaporation method using ultrasound technique. *Colloid and Polymer Science*, 293, 861-873. [\[CrossRef\]](#)
27. Maltesen, M.J., Bjerregaard, S., Hovgaard, L., Havelund, S., van de Weert, M., Grohgan, H. (2011). Multivariate analysis of phenol in freeze-dried and spray-dried insulin formulations by NIR and FTIR. *AAPS Pharmscitech*, 12, 627-636. [\[CrossRef\]](#)
28. Badri, W., Miladi, K., Robin, S., Viennet, C., Nazari, Q.A., Agusti, G., Fessi, H., Elaissari, A. (2017). Polycaprolactone based nanoparticles loaded with indomethacin for anti-inflammatory therapy: From preparation to *ex vivo* study. *Pharmaceutical Research*, 34, 1773-1783. [\[CrossRef\]](#)
29. Zhao, X., Zu, Y., Zu, S., Wang, D., Zhang, Y., Zu, B. (2010). Insulin nanoparticles for transdermal delivery: Preparation and physicochemical characterization and *in vitro* evaluation. *Drug Development and Industrial Pharmacy*, 36(10), 1177-1185. [\[CrossRef\]](#)
30. Diwan, R., Ravi, P.R., Agarwal, S.I., Aggarwal, V. (2021). Cilnidipine loaded poly (ϵ -caprolactone) nanoparticles for enhanced oral delivery: Optimization using DoE, physical characterization, pharmacokinetic, and pharmacodynamic evaluation. *Pharmaceutical Development and Technology*, 26(3), 278-290. [\[CrossRef\]](#)
31. Shinde, T., Agnihotri, T.G., Gomte, S.S., Sharma, N., Jain, A. (2024). Quality by design-driven development of hydroxyurea-loaded polymeric nanoparticles. *BioNanoScience*, 14(3), 2691-2704. [\[CrossRef\]](#)
32. Kumar, A., Sawant, K. (2013). Encapsulation of exemestane in polycaprolactone nanoparticles: Optimization, characterization, and release kinetics. *Cancer Nanotechnology*, 4, 57-71. [\[CrossRef\]](#)
33. Costa, P., Lobo, J.M.S. (2001). Modeling and comparison of dissolution profiles. *European Journal of Pharmaceutical Sciences*, 13(2), 123-133. [\[CrossRef\]](#)

34. Tuğcu-Demiröz, F., Saar, S., Kara, A.A., Yıldız, A., Tunçel, E., Acartürk, F. (2021). Development and characterization of chitosan nanoparticles loaded nanofiber hybrid system for vaginal controlled release of benzydamine. *European Journal of Pharmaceutical Sciences*, 161, 105801. [\[CrossRef\]](#)
35. Suvakanta, D., Padala, N.M., Lilakanta, N., Prasanta, C. (2010). Kinetic modeling on drug release from controlled drug delivery systems. *Acta Poloniae Pharmaceutica*, 67(3), 217-223.